UDC 539.21 (06)

Vestnik SibGAU
Vol. 16, No. 2, P. 485–490

TECHNOLOGY READY USE FOR PRODUCING NANOMATERIALS IN THE PLASMA OF A LOW-PRESSURE PULSED ARC DISCHARGE

A. V. Ushakov[1], I. V. Karpov[1], A. A. Lepeshev[1,2], A. A. Shaihadinov[1], L. Yu. Fedorov[1*]

[1]Siberian Federal University
79, Svobodny Av., Krasnoyarsk, 660041, Russian Federation
[2]Krasnoyarsk Scientific Center, Siberian Branch, Russian Academy of Sciences,
50, Akademgorodok, Krasnoyarsk, 660036, Russian Federation
*E-mail: sfu-unesco@mail.ru

A new method for the production of nanomaterials in the plasma of a low-pressure arc discharge is developed and experimentally studied. This method can be used to synthesize nanoparticles 5-10 nm in size with a narrow size distribution. In this method, a low-pressure arc discharge is used to melt a material, to disperse the molten material, to deliver liquid material droplets to the plasma, to cool the liquid nanoparticles forming in the plasma up to their solidification, and to deposit the solidified nanoparticles onto a substrate.

Keywords: nanomaterials, low-pressure arc discharge, vacuum, zirconium oxide, derivatogram.

Вестник СибГАУ
Т. 16, № 2. С. 485–490

МЕТОД ПОЛУЧЕНИЯ НАНОДИСПЕРСНЫХ МАТЕРИАЛОВ В ПЛАЗМЕ ИМПУЛЬСНОГО ДУГОВОГО РАЗРЯДА НИЗКОГО ДАВЛЕНИЯ

А. В. Ушаков[1], И. В. Карпов[1], А. А. Лепешев[1,2], А. А. Шайхадинов[1], Л. Ю. Федоров[1*]

[1]Сибирский федеральный университет
Российская Федерация, 660041, г. Красноярск, просп. Свободный, 79
[2]Красноярский научный центр Сибирского отделения Российской академии наук
Российская Федерация, 660036, г. Красноярск, Академгородок, 50
*E-mail: sfu-unesco@mail.ru

Разработан и экспериментально исследован новый метод получения нанодисперсных материалов в плазме дугового разряда низкого давления. Разработанный способ позволяет синтезировать нанодисперсные частицы от 5 до 10 nm с узким распределением по размерам. Особенностью разработанного метода является то, что расплавление и диспергирование расплавленного материала, подачу полученных жидких капель этого материала в плазму, охлаждение жидких наночастиц, формируемых в плазме до их отвердевания, и осаждение полученных твердых наночастиц на подложку осуществляют при помощи дугового разряда низкого давления.

Ключевые слова: наночастицы, дуговой разряд низкого давления, вакуум, оксид циркония, дериватография.

Introduction. The following evaporation and condensation methods are used to synthesize nanodispersed powders: laser, electron beam, electric explosion of wires, and so on [1]. We believe that the synthesis of nanomaterials in the plasma of a low-pressure pulsed arc discharge is the most promising method. In this method, an initial substance is mainly generated in a vapor phase and is then transformed into a plasma state due to the erosion of the electrodes of high-current arc discharges [2]. These discharges can have almost any electric power, which opens up fresh opportunities for generating high-density monoplasma (plasma of a solid elementary substance). When such processes are carried out in high vacuum, great possibilities are opened for both direct condensation from monoplasma (in a flow or at a surface) at a high rate and direct synthesis of complex substances from elements (monoplasmas). In this case, chemical reactions are very intense since the degree of plasma ionization is very high (up to 100 %). These methods can be used to synthesize various alloys, oxides, nitrides, and carbides [3–6]. The process purity is determined by the achieved vacuum (no auxiliary atmosphere is required), and the condensation rate can be very high, increasing in proportion to the electric power of the discharge. Moreover, a vacuum arc is one of the most efficient sources of the ions of the metal to be evaporated, which makes it possible to further increase the ionization of a plasma flux due to the ionization of a vapor component. When the plasma flux energy is sufficient, the evaporation of a metal (cathode) in a low-pressure arc discharge has the following two stages: the cathode material is first sprayed in the liquid phase in a cathode spot and is then fully evaporated in a vapor – plasma flux. In addition, the vapors are overheated because of the mixing of metal vapors with the flux of an ionizing carrier gas, which hinders premature vapor condensation and causes the dissociation of formed clusters.

The purpose of this work is to develop and study a method for producing high-quality nanoparticles smaller than 10 nm in size with a dispersion of 1.2 and to deposit a close-packed multilayer coating made of such particles onto a substrate.

Experimental. The proposed method includes the melting and dispersion of a melted cathode material using a low-pressure pulsed arc discharge, the supply of liquid drops of this material to a plasma, the cooling of the liquid nanoparticles formed in the plasma, and the solidification and deposition of solid particles onto a substrate. In this case, the arc discharge pulse duration should be shorter than the time of formation of a continuous liquid bath on a target and, on the other hand, should ensure the introduction of the energy sufficient for material (including refractory material) evaporation and the creation of a vapor density that is sufficiently low to exclude particle coalescence.

In pulsed arc discharges, the ion energy is usually lower than 10 eV and the pulse current does not exceed 3 A. These ion beam parameters are reached if the pulse duration is 20–300 μs. In this case, the cathode current density should be at least 10^8 A/cm^2 for the major portion of the material to be evaporated in the ablation regime [7]. It is impossible to fully exclude the creation of a liquid bath on a target and, hence, the emission of drops from the target due to the physics of absorption of the electron beam energy by the target material, which has a nonlinear character.

Evaporation into a low-pressure gas makes it possible to reach high expansion rates, which ensure a rapid decrease in the vapor coordination number and the formation of small particles. The presence of a gas provides sufficiently rapid cooling–quenching of powder particles due to both radiation heat exchange (as in vacuum) and molecular heat exchange. The lower value of gas pressure can be estimated from the criterion of a substantial fraction of heat losses in particles due to molecular heat exchange. This pressure was estimated to be at least 50 Pa [8–11]. The upper gas pressure can be estimated from the criterion of a stable arc discharge and the possibility of its magnetic stabilization on the cathode surface. This pressure was estimated to be higher than 80 Pa [8].

The cathode vacuum arc plasma mainly consists of ionized and excited cathode material particles. The characteristic property of the cathode vacuum arc is the discharge current density in cathode spots, where the current density, the power density, the plasma density, and the plasma pressure can reach 100 A/cm^2, 10^9 W/cm^2, 10^{20} cm^{-3}, and 10^{10} Pa, respectively, due to small arc spots (~10 μm) and a short spot lifetime (~10^{-7} s).

The formation of cathode spots results from explosive electron emission from (geometric and structural) cathode surface microasperities. It is characteristic that cathode spots move arbitrarily or under the action of an external magnetic field and form craters several or several tens of microns in diameter. These craters to a great extent result from the splashing of the material melted under the action of plasma pressure and serve as the sources of liquid drops 0.1–1 in size [12; 13].

The dense erosion plasma of a cathode spot in which drops fly has a rather high temperature because of an extremely high power density in the cathode spot; therefore, this plasma is completely ionized and contains both singly and multiply ionized ions [14].

A high energy concentration leads to explosive fracture of the cathode, which is accompanied by explosive electron emission. The splashing of a liquid metal in the form of drops and streams from a cathode spot occurs under the action of the reactive force that appears during the expansion of high-speed plasma jets, which is characteristic of short high-current arcs. Moreover, the rejection of a liquid metal to the periphery of the melt, where it is removed in a drop phase, can be explained by the thermocapillary effect caused by the temperature dependence of the surface tension of the melt.

The situation where a drop passes into a plasma jet, is overheated, and transforms into vapor can appear because of the large difference between the expansion velocities of plasma jets and drops.

Thus, our estimate shows that, at a sufficient plasma jet energy, the evaporation of a cathode in a low-pressure arc discharge has the following two-stage character: the cathode material first splashes as a liquid phase in a cathode spot and then fully evaporates in a near-electrode vapor-gas mixture. Moreover, the vapors are overheated due to the mixing of the metal vapors with the flux of an ionized carrier gas, which prevents premature vapor condensation and induces the dissociation of formed clusters.

The method was used to synthesize nanodispersed ZrO_2 on a special-purpose electric arc dispersion setup, where nanoparticles are formed using a vacuum arc discharge as a source of plasma and drops (fig. 1).

A pulsed arc evaporator of a metal is located in a vacuum chamber. This evaporator consists of a cylindrical cooled consumable electrode with attached current leads for power supply and cooling liquid supply, a coaxial cooled anode attached to the cathode with a fluoroplastic insulator, a magnetic bias system inside the anode, a flange attached to the chamber wall and to the anode with fluoroplastic insulators, and an anode combined with a cylindrical cooled condensation surface that can rotate about the cathode, and an igniter electrode with attached current leads. A pilot arc is powered with electric power supply the minus of which is connected through the magnetic bias system to current leads and the plus of which is connected to the coaxial anode. A pulsed high-current arc is powered with electric power supply the common wire of which is connected to the anode, and negative pulses are supplied through the magnetic bias system to current leads. A mechanism for the removal of the forming powder is placed near the condensation surface. A bunker is situated in the lower part of the vacuum chamber to collect the powder. The lower part of the vacuum chamber also has a reaction gas feeding system.

Results and discussion. The developed method was implemented as follows. As the cathode for spraying, we used commercial-purity E 100 zirconium. For plasma-chemical reactions to occur, a 5 % O_2 + 95 % Ar gas mixture was let in the chamber preliminarily pumped out to a pressure of 1.33×10^{-3} atm. Synthesis was performed at a gas mixture pressure of 60 Pa. A pulsed arc discharge with a frequency of 1 kHz, a pulse duration of 250 µs, and a pulsed current amplitude of 2.3 kA was maintained with power supply.

The magnetic bias system is included into the current circuit of the cathode and is used to stabilize the operation of the arc evaporator. Melting of the material and its dispersion into drops occur in the crater of a cathode spot. Formed drops pass to the dense erosion plasma of a cathode spot. As a result, all drops are charged and heated due to collisions with electrons at least to the critical value of the beginning of their cascade division in the time of flight in the cathode spot plasma. The formed nanoparticles are cooled to solidification in the rapidly expanding cathode spot plasma and the interelectrode discharge plasma in a time of about 10^{-7} s, which results in amorphization of their structure. During the evaporation of the cathode material in the arc discharge, the nanoparticle flux reaches the rotating cooled surface and deposits on it in the form of a powder. A zirconium oxide nanopowder formed in 10 min and was then accumulated in the bunker.

The morphological composition of the powder was studied on a JEOL JEM-2100 transmission electron microscope. A ZrO_2 sample for an electron-microscopic investigation was prepared as follows: the powder was located in isopropyl alcohol and dispersed in an ultrasonic bath for 2 min, and a solution drop was then placed on a carbon film substrate situated on an electron-microscopic supporting grid. The carbon film substrate thickness was 10–15 nm.

The synthesized zirconium oxide nanopowder was light gray. Fig. 2 shows a typical photograph of the zirconium oxide nanopowder. The average particle size is 5 nm and particles 6–7 nm in size can also exist. As a rule, the particle shape is close to a spherical one. The nanoparticles have a crystalline structure, which is indicated by atomic planes observed in images. The investigation of the granulometric composition showed that the prepared nanopowder has a lognormal distribution, the average geometric particle size was d_g = 5.7 nm, the average mass particle size was d_m = 5.9 nm, and the dispersion was a_g = 1.2. The maximum specific surface for the zirconium oxide nanopowder was 470 m^2/g. The chemical composition of the ZrO_2 powder is given in the table.

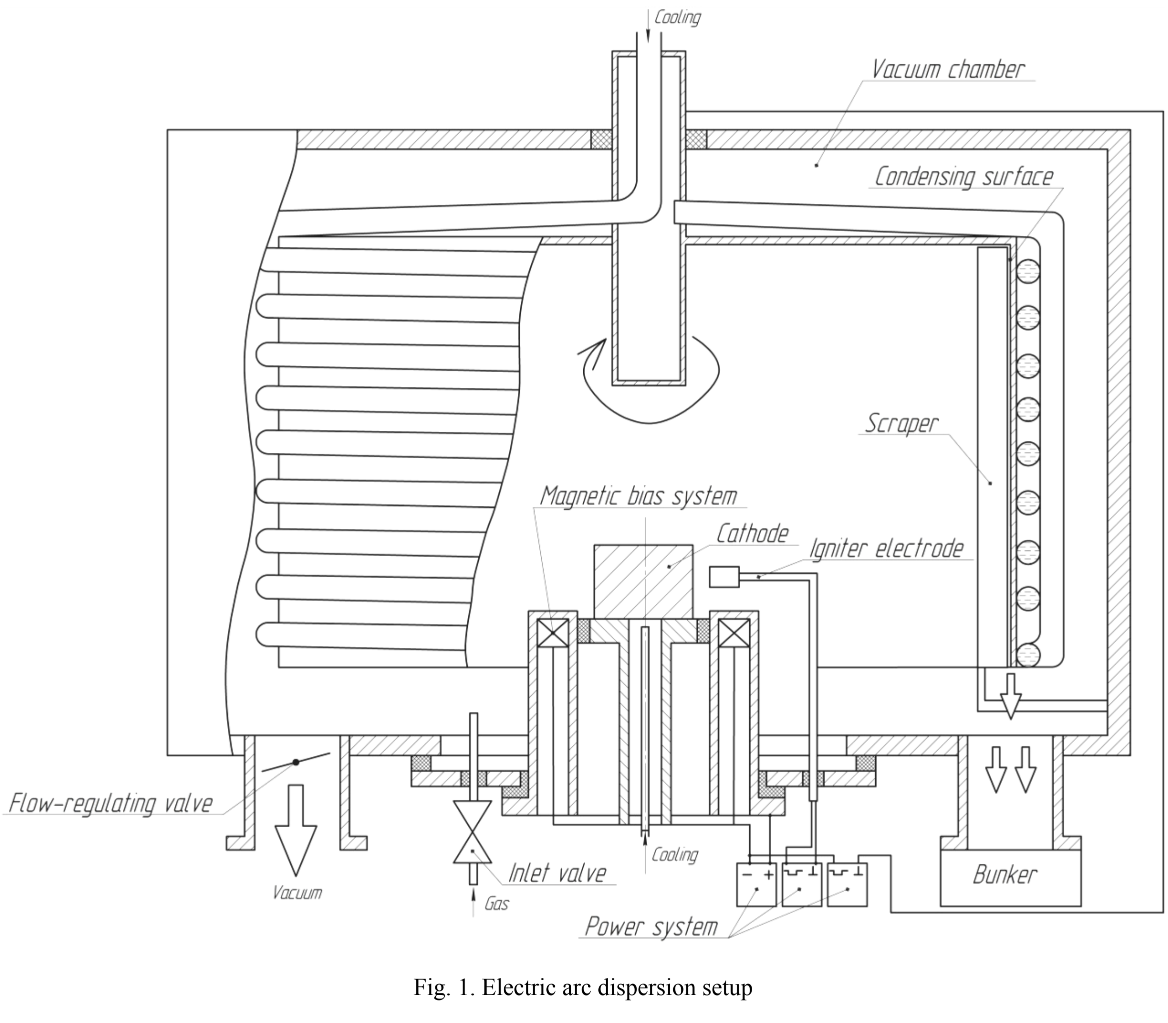

Fig. 1. Electric arc dispersion setup

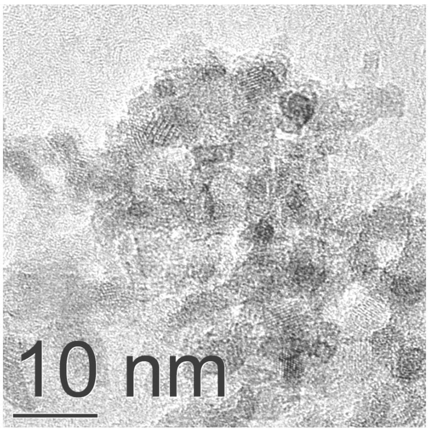

Fig. 2. Micrograph of the zirconium oxide nanopowder

The phase composition of the powder was analyzed by X-ray diffraction (XRD) with an Advance D8 diffractometer using monochromatized CuK$_a$ radiation. Scanning was carried out at room temperature in the 2θ angular range 5°–120° at a step of 0.04°.

The microstructure characteristics and the unit cell parameters were determined using the Rietveld full-profile analysis of X-ray diffraction patterns [15]. We used a software package based on a modified and corrected version of the DBWS-9006PC structure refinement program using the Rietveld method [16].

Chemical composition of a zirconium dioxide nanopowder

ZrO_2	
Element	Content, wt %
Zr	70.16
O	29.7
Si	0.02
Cr	0.02
Fe	0.04
Cu	0.04
Zn	0.02

The XRD results for the zirconium oxide powder are shown in fig. 3. When annealed at 690 K for 2 h, the zirconium oxide powder crystallizes into the tetragonal lattice corresponding to the baddeleyite structure (fig. 4). The average crystallite size is 5 nm. In contact with atmosphere, the zirconium oxide powder weight increases in 2–3 min. The maximum change in the zirconium oxide powder weight was 18 wt %.

The zirconium oxide powders formed in the plasma of a low-pressure pulsed arc discharge have a rather low bulk density, which relatively weakly depends on the specific surface area in the dispersion range under study (up to 470 m^2/g) and strongly depends on the methods of subsequent treatment of the powders. As a rule, the as-prepared powders have the minimum bulk density, which is 0.04 g/cm^3 for zirconium oxide.

The synthesized nanopowders were subjected to thermal analysis. The sample mass was 100 mg. Zirconium oxide nanopowder samples were heated in the temperature range from 291 to 1273 K at a rate of 10 K/min. The experimental results are presented in fig. 5 and 6. Water evaporates intensely from zirconium oxide nanopowders in the temperature range 343–423 K, which is indicated by a decrease in the sample mass by 4 wt % in a thermogravimetric curve in spite of the fact that the corresponding differential thermal analysis curve has no pronounced maximum.

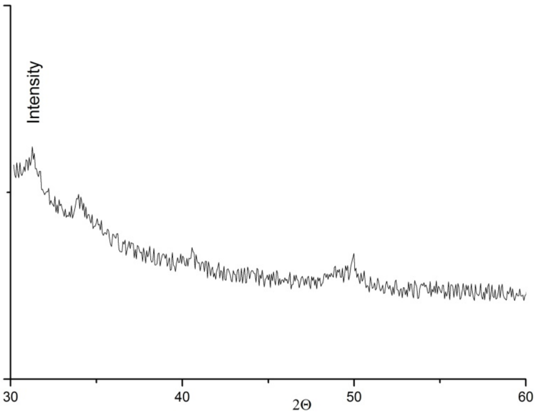

Fig. 3. X-ray diffraction pattern of the zirconium oxide nanopowder

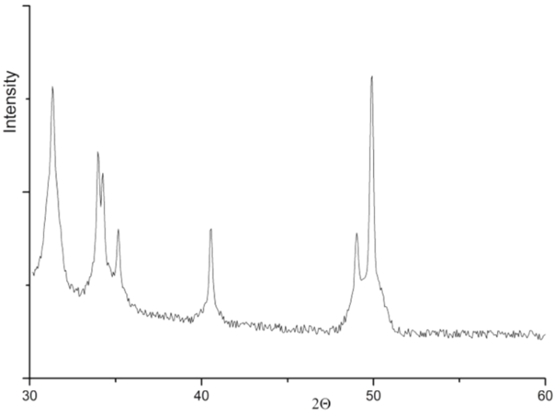

Fig. 4. X-ray diffraction pattern of the ZrO_2 sample annealed at 690 K for 2 h

The experimental results demonstrate that the zirconium oxide powder produced in a low-pressure arc discharge has a particle size smaller than 10 nm with a very narrow particle size distribution. The specific surface area suggests that a condensate with a particle size that is significantly smaller than in the base powder deposits on the particle surfaces. This condensate forms a porous “coat” around particles and substantially determines the chemical activity of the powder, which explains the high sorption activity of the powder with respect to atmospheric moisture. The optimum powder synthesis conditions are determined by the gas mixture pressure. XRD studies demonstrate that particles with both an amorphous and a crystalline structure can be synthesized when the cooling rate of the vapor-plasma flux is controlled. The phase composition of nanopowders can be controlled from nonmetal nonstoichiometry to metal nonstoichiometry. The results of investigating the oxidation of an electric arc zirconium powder in air showed that a decrease in the particle size leads to a decrease in the reactivity of the powder at room temperature.

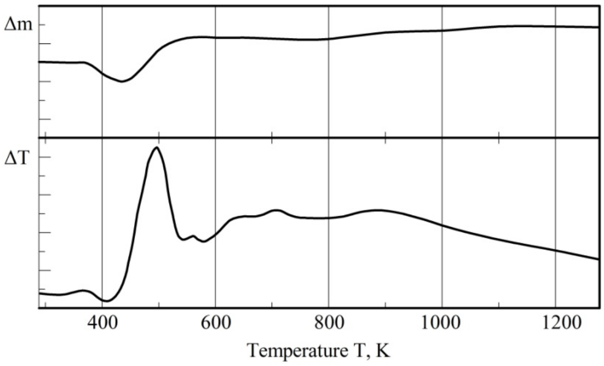

Fig. 5. Derivatogram of heating the electric arc zirconium oxide powder

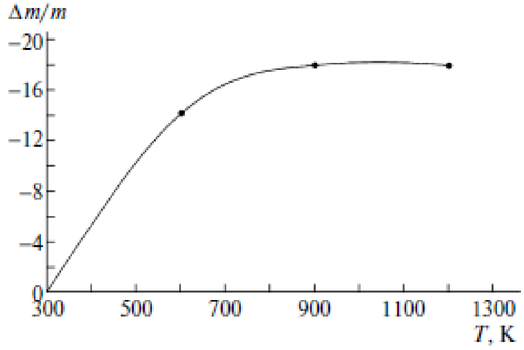

Fig. 6. Thermogravimetric curve of heating the zirconium oxide nanopowder in air

Conclusion. When comparing the experimental results obtained for titanium nitride [8] with the results obtained for zirconium oxide, we can conclude that the proposed method for producing nanopowder in the plasma of a low-pressure arc discharge is universal. This method is characterized by high manufacturability and low energy consumed for the production of a unit of output, since the total time of nanodrop generation is the statistical superposition of such processes in individual cathode spots moving spontaneously (or under the action of a magnetic field) over the cathode surface. This continuous formation of cathode spots ensures uniform cathode erosion, which results in an increase in the lifetime of the cathode and the entire setup. Although the formation of nanoparticles in the plasma of an individual cathode spot is a pulsed process ($t_p \sim 10^{-7}$ s), the operation of the setup used to implement the proposed method can be characterized as a highly productive stationary process with the continuous operation resource determined by the cathode material lifetime (100 h or more).

The produced zirconium oxide powders have an amorphous-crystalline monophase structure and a narrow granulometric composition with an average particle size of 5 nm.

Acknowledgments. This work was partly supported by the Ministry of Education and Sciences of the Russian Federation (projects no. 11.370.2014/K, 11.1287.2014/K).

Благодарности. Данная работа выполнена при частичной финансовой поддержке Министерства образования и науки Российской Федерации (проекты № 11.370.2014/K, 11.1287.2014/K).

References

1. Gusev A. I. *Nanomaterialy, nanostruktury, nanotekhnologii* [Nanomaterials, Nanostructures, Nanotechnology]. Moscow, Fizmatlit Publ, 2005. 416 p.
2. Mesyats G. A., Proskurovsky D. I. *Pulsed Electrical Discharge in Vacuum.* Berlin, Springer, 1989, 293 p.
3. Saunin V. N., Telegin S. V. [Plasma Spraying Ferrite Coverage] *Vestnik SibGAU*, 2014, No. 1 (53), P. 168–174 (In Russ.).
4. Gordeev Ju. I., Abkarjan A. K., Jasinskij V. B., Binchurov A. S., Vadimov V. N. [Design and Research Nanostructured firm alloys Composites with High Level Strength and Operational Performance by Modifying Nanoparticles and Thermomechanical Processing] *Vestnik SibGAU*, 2014, No. 4 (56), P. 209–218 (In Russ.).
5. Miheev A. E., Girn A. V., Ivasev S. S., Evkin I. V. [Investigation of Coatings for the Spacecraft] *Vestnik SibGAU*, 2013, No. 3 (49), P. 217–224 (In Russ.).
6. Takamasa Ishigaki, Ji-Guang Li. Synthesis of functional TiO_2-based nanoparticles in radio frequency induction thermal plasma. *Pure Appl. Chem.*, 2008, Vol. 80, No. 9, P. 1971–1979. doi: 10.1351/pac200880091971.
7. Barengol’ts S. A., Mesyats G. A., Shmelev D. L. Mechanism of ion flow generation in vacuum arcs. *JETP*, 2001, Vol. 93, No. 5, P. 1065–1073. doi:10.1134/1.1427117.
8. Ushakov A. V., Karpov I. V., Lepeshev A. A., Krushenko G. G. [Physico-chemical properties nanomodifiers based arc titanium nitride powder for polymer nanocomposite materials] *Tekhnol. Met.* 2011, No. 3, P. 16–21 (In Russ.).
9. Karpov I. V., Ushakov A. V., Fedorov L. Yu., Lepeshev A. A. Method for Producing Nanomaterials in the Plasma of a Low Pressure Pulsed Arc Discharge. *Tech. Phys.*, 2014, Vol. 84, No. 4, P. 559–563, doi: 10.1134/S1063784214040148.
10. Fedorov L. Yu., Karpov I. V., Ushakov A. V., Lepeshev A. A. Influence of Pressure and Hydrocarbons on Carbide Formation in the Plasma Synthesis of TiC Nanoparticles. *Inorganic Materials*, 2015, Vol. 51, No. 1, P. 25–28, doi: 10.1134/S0020168515010057.

11. Ushakov A. V., Karpov I. V., Fedorov L. Yu., Lepeshev A. A. Mechanical and Tribological Properties of Complex-Modified Material Based On Ultra High Molecular Weight Polyethylene. *Journal of Friction and Wear*, 2014, Vol. 35, No. 1, P. 7–11, doi: 10.3103/S1068366614010103.

12. Anders A. The fractal nature of vacuum arc cathode spots. *IEEE Trans. Plasma Sci.*, 2005, Vol. 33, No. 5, P. 1456–1464, doi: 10.1109/TPS.2005.856488.

13. Anders A. Metal plasma immersion ion implantation and deposition: a review. *Surf. Coat. Technol.*, 1997, Vol. 93, No. 2–3, P. 158–167, doi: 10.1016/S0257-8972(97)00037-6.

14. Krinberg I. A. The ion charge-current strength relationship in stationary and pulsed vacuum discharges. *Tech. Phys. Lett.*, 2001, Vol. 27, No. 1, P. 45–48, doi: 10.1134/1.1345162.

15. Rietveld H. M. Profile Refinement Method for Nuclear and Magnetic Structures. *J. Appl. Crystallogr.*, 1969, No. 2, P. 65–71. doi:10.1107/S0021889869006558.

16. Wiles D. B. New Computer Program for Rietveld Analysis of X-ray Powder Diffraction Patterns. *J. Appl. Crystallogr.*, 1981, No. 14, P. 149–151, doi: 10.1107/S0021889881008996.

Библиографические ссылки

1. Гусев А. И. Наноматериалы, наноструктуры, нанотехнологии. М. : Физматлит, 2005. 416 с.

2. Месяц Г. А., Проскуровский Д. И. Импульсный электрический разряд в вакууме. Новосибирск : Наука, 1984. 256 с.

3. Саунин В. Н., Телегин С. В. Плазмонапыленные ферритовые покрытия // Вестник СибГАУ. 2014. № 1 (53). С. 168–174.

4. Конструирование и исследование наноструктурированных твердосплавных композитов с повышенным уровнем прочностных и эксплуатационных характеристик за счет модифицирования наночастицами и термомеханической обработки / Ю. И. Гордеев [и др.] // Вестник СибГАУ. 2014. № 4 (56). С. 209–218.

5. Исследование свойств защитных покрытий для космических аппаратов / А. Е. Михеев [и др.] // Вестник СибГАУ. 2013. № 3 (49). С. 217–224.

6. Takamasa Ishigaki, Ji-Guang Li. Synthesis of functional TiO_2-based nanoparticles in radio frequency induction thermal plasma // *Pure Appl. Chem.* 2008. Vol. 80, no. 9. P. 1971–1979. Doi: 10.1351/pac200880091971.

7. Barengol'ts S. A., Mesyats G. A., Shmelev D. L. Mechanism of ion flow generation in vacuum arcs // *JETP*. 2001. Vol. 93, no. 5. P. 1065–1073. Doi: 10.1134/1.1427117.

8. Физико-химические свойства наномодификаторов на основе электродуговых порошков нитрида титана для полимерных нанокомпозитных материалов / А. В Ушаков [и др.] // Технология металлов. 2011. № 3. С. 16–21.

9. Method for Producing Nanomaterials in the Plasma of a Low Pressure Pulsed Arc Discharge / I. V. Karpov [et al.] // *Tech. Phys*. 2014. Vol. 84, no. 4. P. 559–563. Doi: 10.1134/S1063784214040148.

10. Influence of Pressure and Hydrocarbons on Carbide Formation in the Plasma Synthesis of TiC Nanoparticles / L. Yu. Fedorov [et al.] // *Inorganic Materials*. 2015. Vol. 51, no. 1. P. 25–28. Doi: 10.1134/S0020168515010057.

11. Mechanical and Tribological Properties of Complex-Modified Material Based On Ultra High Molecular Weight Polyethylene / A.V. Ushakov [et al.] // *Journal of Friction and Wear*. 2014. Vol. 35, no. 1. P. 7–11. Doi: 10.3103/S1068366614010103.

12. Anders A. The fractal nature of vacuum arc cathode spots // *IEEE Trans. Plasma Sci*. 2005. Vol. 33, no. 5. P. 1456–1464. Doi: 10.1109/TPS.2005.856488.

13. Anders A. Metal plasma immersion ion implantation and deposition: a review // *Surf. Coat. Technol.* 1997. Vol. 93, no. 2–3. P. 158–167. Doi: 10.1016/S0257-8972(97)00037-6.

14. Krinberg I. A. The ion charge-current strength relationship in stationary and pulsed vacuum discharges // *Tech. Phys. Lett.* 2001. Vol. 27, no. 1. P. 45–48. Doi: 10.1134/1.1345162.

15. Rietveld H. M. Profile Refinement Method for Nuclear and Magnetic Structures // *J. Appl. Crystallogr.* 1969, no. 2. P. 65–71. Doi: 10.1107/S0021889869006558.

16. Wiles D. B. New Computer Program for Rietveld Analysis of X-ray Powder Diffraction Patterns // *J. Appl. Crystallogr.* 1981, no. 14. P. 149–151. Doi: 10.1107/S0021889881008996.